Hindawi
International Journal of Antennas and Propagation
Volume 2022, Article ID 1017816, 7 pages
https://doi.org/10.1155/2022/1017816

Research Article

An On-Chip Planar Inverted-F Antenna at 38 GHz for 5G Communication Applications

Syed Muhammad Ammar Ali

Department of Engineering, Massey University, Albany, Auckland 0632, New Zealand

Correspondence should be addressed to Syed Muhammad Ammar Ali; s.ali2@massey.ac.nz

Received 13 March 2022; Revised 25 April 2022; Accepted 28 April 2022; Published 8 June 2022

Academic Editor: Eng Hock Lim

Copyright © 2022 Syed Muhammad Ammar Ali. This is an open access article distributed under the Creative Commons Attribution License, which permits unrestricted use, distribution, and reproduction in any medium, provided the original work is properly cited.

This paper presents an on-chip planar inverted-F antenna (PIFA) implemented in TSMC 180 nm CMOS process technology. The antenna operates at a 5 G millimeter-wave center frequency of 38 GHz. The ultrathick metal (UTM) layer of the technology is utilized to implement the on-chip antenna (OCA). The OCA is positioned close to the edge of the microchip for improving the gain performance of the antenna. The open end of the antenna is folded to develop a top-loaded PIFA structure yielding better 50 Ω impedance matching and wider bandwidth. On-wafer measurements are conducted through the Cascade Microtech Summit 11K probe-station and ZVA-50 vector network analyzer to measure the return loss and gain of the fabricated on-chip antenna. The measurements are performed after placing the fabricated OCA over a 3D-printed plastic slab to minimize the reflections from the metallic chuck of the probe station. The measurement results show that the fabricated on-chip PIFA achieves a minimum return loss of 14.8 dB and a gain of 0.7 dBi at the center frequency of 38 GHz. To the best of the authors' knowledge, the presented OCA is the first on-chip PIFA designed, fabricated, and tested at the 5G millimeter-wave frequency of 38 GHz.

1. Introduction

The millimeter-wave frequencies have recently gained enormous attention among research circles because of their capability of providing high data rates for 5 G communication systems. As millimeter-wave (mmW) frequencies exhibit relatively smaller wavelengths, therefore, it becomes feasible to design antennas on microchips using standard CMOS processes. Millimeter-wave on-chip antennas (OCAs) offer a high level of integration with RF front-end circuitry, external interconnect-free interface, and low fabrication cost. The on-chip antenna (OCA) can overcome the last barrier to realize a truly integrated RF system [1]. A potential candidate for next-era cellular communications at millimeter-wave frequencies is 38 GHz due to its minimum atmospheric absorption characteristics [2]. Therefore, in this work, a 5 G millimeter-wave frequency of 38 GHz is selected for designing an on-chip antenna.

Several on-chip antenna structures have been proposed in the literature, and most of these OCAs were designed to operate at the millimeter-wave frequency of 60 GHz. A couple of on-chip PIFA has been proposed in the literature. In [3], a straight-line PIFA fabricated in standard CMOS process technology was proposed. The OCA was operable at a millimeter-wave frequency of 60 GHz. The antenna was excited at the fourth-order mode resulting in an increased antenna footprint. The measurement results showed that the OCA yielded an absolute gain of −19 dBi. A PIFA has a very strong dependence on the ground plane, and the OCA in [3] was designed without a ground plane thereby causing significant deterioration in antenna gain. A meander-line on-chip PIFA fabricated in TSMC 180 nm CMOS process technology was proposed in [4]. The OCA was excited at a 5G millimeter-wave frequency of 60 GHz and produced an absolute gain value of −15.7 dBi. The OCA's meandered section, residing at the edge of the microchip, helped to reduce the overall antenna length; however, a considerable part of the antenna body remained away from the edge of the microchip causing reduction in radiation efficiency. Moreover, the work did not show the dimensions of the

antenna thereby providing no information on the width and length of the fabricated OCA. A 60-GHz triangular monopole antenna-on-chip in 180 nm CMOS process technology was designed in [5]. The gain of the antenna was attempted to be improved with the help of artificial magnetic conductors (AMCs). Simulation results showed that the antenna produced a gain of 2.5 dBi. A 60 GHz on-chip patch antenna in 180-nm CMOS technology was presented in [6]. The measurement results indicated that the antenna offered a gain performance of around −2.2 dBi in the frequency range between 50 and 70 GHz. Very recently, a monopole on-chip antenna fabricated in 65-nm CMOS technology was proposed in [7]. The OCA reported an antenna gain of 0-dBi at 60-GHz. Apart from the above-mentioned OCAs, there were several other OCAs excited at the millimeter-wave frequency of 60 GHz [8–11]; however, a 38-GHz triangular monopole on-chip antenna was reported in [12]. The OCA was designed with AMCs in 28 nm CMOS process technology. The work presented simulation results only. The OCA showed an antenna gain of −1.75 dBi and occupied a considerably huge area of more than 4 mm^2 on the microchip. The metal width of the OCA was 8 μm which is very narrow and thus contributed to constraining the antenna gain. Moreover, the simulation-based OCA did not discuss the requirements of the metal-fill density and the practical feasibility or nonfeasibility of such a large (more than 4 mm^2) exclusion area, essential for the proper operation of the antenna on the microchip. In simulations related to on-chip antennas, exclusion area limitation may opt to be ignored by the designer, but practically the scenario appears to be quite different.

A large metallic area like a patch or similar structure constructed using the top-most metal layer of CMOS technology has the potential to suffer microfracture; hence, in this work, a planar inverted-F antenna comprising of a few metallic lines is selected to avoid such a risk. Moreover, a favorable feature of PIFA with regard to on-chip integration is its small vertical dimension. It enables the antenna to be implemented at one of the chip's edges thereby facilitating the antenna to radiate readily in the free space and hence minimizing the absorption of electromagnetic radiation within the silicon substrate. As PIFA has both horizontal and vertical elements, therefore, it can perform in both horizontal and vertical polarizations. The performance of PIFA with two-polarizations helps to improve the reception in WPAN environments. The input impedance of a PIFA can be set by adjusting the distance between the shorting stripe and the feeding stripe. The input impedance can be tuned to an appropriate value to match the source impedance without making use of an additional circuit between the source and the antenna. PIFA offers a small form factor as it is only a quarter wavelength long, and therefore, it can easily fit inside an already space-constraint environment of a microchip. Moreover, a PIFA has a strong connection with the ground plane through its shorting stripe; therefore, as compared to other antennas, it naturally behaves in a very robust manner when operating close to metallic objects, which have the tendency to affect the radiation capabilities of an antenna. This fact is particularly important in a microchip environment where a design rule check (DRC) called as "pattern density" is a ritual that needs to be satisfied. Therefore, a PIFA can better tolerate the presence of the metal-fill chunks in its vicinity as compared to the other OCA designs. After taking all of the above-mentioned facts into account, it can be inferred that a PIFA is the best-suited OCA candidate for indoor 5G-wireless applications. Moreover, due to PIFA's proven edge over other antennas, it is practically being widely used as a mobile communication antenna. However, such an antenna has not been investigated/implemented on-chip at 38 GHz, which is one of the potential 5G frequencies. This work presents a top-loaded on-chip planar inverted-F antenna (PIFA) operable at the millimeter-wave frequency of 38 GHz. The proposed antenna shows a reflection coefficient $|S_{11}|$ value of −14.8 dB and offers an antenna gain of 0.7 dBi at the center frequency of 38 GHz. To the best of the authors' knowledge, this work proposes the first on-chip PIFA designed, fabricated, and tested at the 5 G millimeter-wave frequency of 38 GHz.

This paper is organized as follows. Section 2 describes the details of the CMOS technology and the design of the proposed on-chip PIFA along with the layout challenges. Measurement results are reported in Section 3, and finally, Section 4 concludes the work presented in this paper.

2. On-Chip Planar Inverted-F Antenna Design

The proposed on-chip planar inverted-F antenna (PIFA) is implemented in TSMC 180-nm CMOS process technology. Figure 1 shows the stacked back-end-of-line (BEOL) metal layers of the technology which offers 6 metallization levels. The top-most metal layer M-6 is utilized to implement the on-chip antenna (OCA). There is a passivation layer of silicon nitride which is deposited at the top of the microchip for protection purposes. Silicon substrate is 300 μm thick with permittivity of 11.9 and resistivity of 10 Ω-cm. The region between the metal layer M-6 and the substrate is filled with silicon dioxide having a dielectric constant of 3.9.

The proposed on-chip PIFA design is shown in Figure 2. The antenna consists of a feeding stripe, a shorting stripe, main antenna body, and a folded-stripe section. The structure of the antenna is positioned very close to the edge of the microchip enabling the OCA to radiate readily into the free space and hence minimizes the absorption of radiation within the silicon substrate. The placement of the OCA close to the chip's edge improves the gain performance of the antenna. By varying the effective length ($L_1 + L_2 + L_3 + H$) of the PIFA, the resonant frequency can be tuned. The input impedance of the antenna can be matched to 50 Ω by adjusting the spacing between the feeding and the shorting stripes. The open end of the PIFA is folded to achieve a top-loaded structure. The folded section provides an additional capacitance effect. This capacitance helps to achieve wide bandwidth and improved 50 Ω matching.

As a PIFA is a quarter-wavelength antenna, therefore, the approximate length of the proposed antenna can be evaluated by using the following formula:

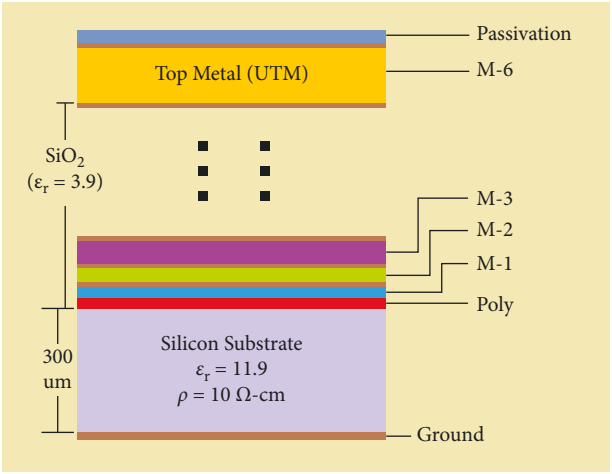

Figure 1: Stacked BEOL metal layers of the TSMC 180 nm CMOS process technology.

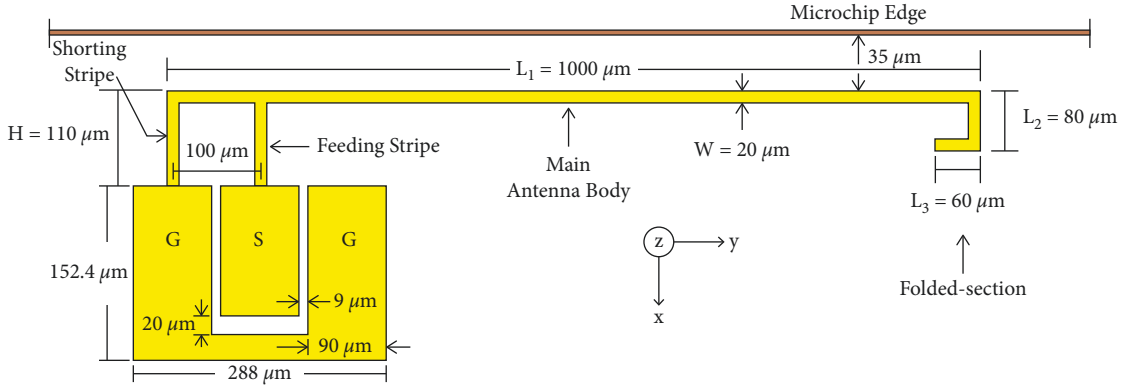

Figure 2: Design and dimensions of the proposed on-chip PIFA.

$$L \approx \frac{\lambda_g}{4} = \frac{1}{4} \cdot \frac{c}{f\sqrt{\varepsilon_r}}, \qquad (1)$$

$$L \approx 1000\mu m,$$

where "λ_g" is guided wavelength. The dimensions of the PIFA were optimized as shown in Figure 3. The blue-colored trace in the figure was captured when the height of the antenna was 100 μm and the open end of the PIFA was not folded whereas the green-colored trace was obtained along with the folded section of the antenna. A clear improvement in terms of reflection coefficient values and bandwidth can be observed in the green trace as compared to the blue trace. However, the green-colored trace was still offset from the desired resonant frequency of 38 GHz. A slight increase of 10 μm in the height of the PIFA centered the resonance dip (red-colored trace) at exactly 38 GHz along with relatively providing an increase of around 1 GHz in the bandwidth of the antenna.

The antenna is fed with the help of a coplanar waveguide (CPW) incorporating 100 μm pitch ground-signal-ground (GSG) pads as shown in Figure 2. As the coplanar waveguide

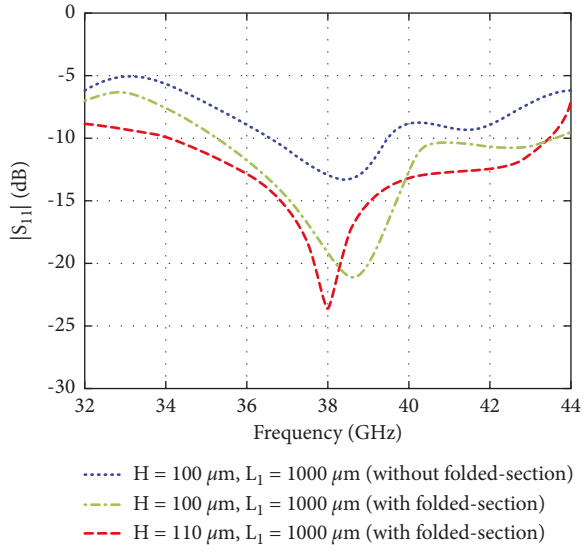

Figure 3: Reflection coefficient traces show a selection of the optimized dimensions of the proposed OCA.

is part of the overall antenna structure, therefore, its effect is involved in the impedance matching characteristics of the antenna. Figure 4 shows the top view of the optimized on-chip antenna. The proposed PIFA is printed by the topmost metal layer M-6, and the ground plane is deployed on the metal layer M-1. In the 180-nm CMOS process node, the top-most metal layer M-6 comes with a few options with regard to the layer thickness. The first one is the general option providing a thickness of 0.99 μm, and the second option is relatively a thicker metal layer with a thickness of 2.34 μm whereas the third option offers the thickest layer called as an ultrathick metal (UTM) layer with 4.6 μm of thickness. In this work, the 4.6 μm UTM is used to implement the antenna structure. The 20-μm-wide metal width of the OCA stripes along with the maximum thickness (4.6 μm) contributes to enhancing the gain performance of the antenna. The ground pads of the proposed antenna are connected to the ground plane at metal layer $M-1$ with the help of vias. The optimized ground plane covers an area of 1645 μm × 897 μm as shown in Figure 4. The ground plane reflects the electromagnetic radiation and thereby improves the antenna gain.

There is an important practical consideration regarding standard foundry fabrication rules which needs to be taken into account while designing an integrated antenna in standard CMOS processes. Fabrication rules also termed as "design rule check" (DRC) are imperative to be satisfied for deploying any structure on the silicon substrate for manufacturability. The DRC of concern for the OCA is "pattern density". Pattern density means that all the metal layers of that process technology need to satisfy a specific percentage (20% to 80%) of the metal-fill in the total area of the microchip. However, these small chunks of every metal layer spread all around the microchip will cause disturbance in the electromagnetic radiation from the integrated antenna. Therefore, in order to avoid the metal-fill interference, an exclusion area (0.439 mm^2) in the layout is designed surrounding the PIFA structure as shown in Figure 4.

Mostly, on-chip antennas (OCAs) designed at 60-GHz have deployed artificial magnetic conductors (AMCs) underneath the antenna structure; however, AMCs at 38 GHz are practically nonfeasible on the chip due to the constraint of the large exclusion area. At high mmW frequencies (like 60-GHz), the dimensions of the AMC unit cell are small whereas, at relatively low mmW frequencies (like 38-GHz), these dimensions become comparatively large. Therefore, the overall AMC grid designed at the mmW frequency of 38-GHz will occupy a huge area on the microchip and, hence, for the purpose of ensuring effective operation, will demand all its occupied regions to be excluded from the dummy metal-fill. However, at the fabrication end, the microchip foundries do not allow a large exclusion area due to the high possibility of microfractures in the chip and/or deformation of the microchip structure. In fact, a large exclusion area jeopardizes the mechanical stability of the microchip and, hence, is not approved by the foundry.

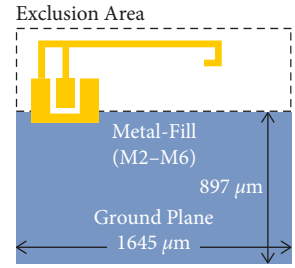

Figure 4: Top view of the proposed OCA depicting designated exclusion area along with dummy metal-fill region and the ground plane.

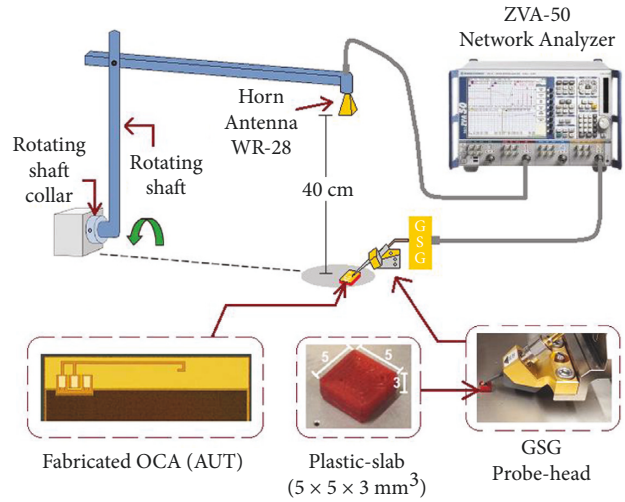

Figure 5: Radiation pattern measurement setup of the antenna under test (AUT) employing Cascade Microtech GSG coplanar probe, WR-28 horn antenna, and Rohde & Schwarz ZVA-50 vector network analyzer.

3. Antenna Measurement Results

The photomicrograph of the on-chip planar inverted-F antenna (PIFA) implemented in TSMC 180 nm CMOS process technology is shown in Figure 5. The area occupied by the antenna on the microchip is 1645 μm × 1164 μm. Cascade Microtech Summit 11K probe station and Rohde & Schwarz (ZVA-50) vector network analyzer (VNA) are used to perform the on-wafer measurements. The Cascade Microtech coplanar probes are landed on 100 μm-pitch GSG (ground-signal-ground) pads for the purpose of exciting the antenna. The reflection coefficient $|S_{11}|$ of the proposed OCA is shown in Figure 6. Simulated and measured reflection coefficient values are −23.76 dB and −14.8 dB, respectively, at the center frequency of 38 GHz. The figure shows that the measured reflection coefficient trace stays below −10 dB for a considerable range of frequencies. It can also be observed from Figure 6 that the measured resonance dip has shifted to about 2 GHz from the simulated resonance dip. The reason for this shift could be that the introduced signal has perceived the longitudinal dimension of the antenna as slightly smaller than the realized stripe.

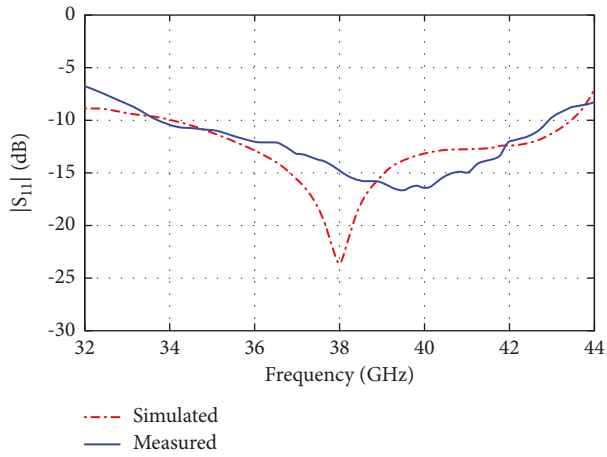

FIGURE 6: Simulated and measured reflection coefficient $|S_{11}|$ of the on-chip PIFA.

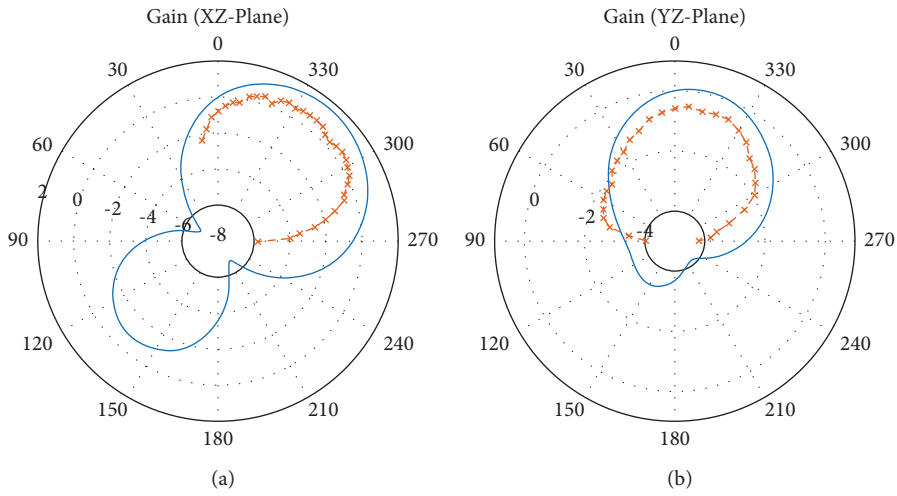

FIGURE 7: Simulated (blue) and measured (orange) radiation patterns in the *XZ* plane (a) and *YZ* plane (b) at the center frequency of 38 GHz.

Figure 5 depicts the test setup for antenna gain and radiation pattern measurements. The antenna under test (AUT) senses the radiation from the WR-28 standard gain horn antenna (26.5–40 GHz) with a gain of 15 dBi. The aperture dimensions of the horn antenna are $19.03 \times 13.64\ \text{mm}^2$. The rotating shaft is steered at different angles to trace the radiation pattern of the AUT. For radiation-gain calculation through Friis transmission expression, the transmission coefficient $|S_{21}|$ is measured between the horn antenna and the AUT with the help of a vector network analyzer. The distance between the AUT and the horn antenna is kept as 40 cm to ensure the far-field criteria, expressed by the following formula:

$$R \geq \frac{2D^2}{\lambda_0}, \tag{2}$$

where D is the largest aperture dimension of the horn antenna and λ_0 is the free-space wavelength.

The antenna gain is calculated by the help of the following formula:

$$[G_{\text{AUT}}]_{dB} = [S_{21}]_{dB} - [G_{\text{Horn}}]_{dB} + [L_{\text{Probe}}]_{dB} + [L_{\text{Adapter}}]_{dB} - \left[\left(\frac{\lambda}{4\pi R}\right)^2\right]_{dB}, \tag{3}$$

where S_{21} is transmission coefficient, G_{Horn} is gain of the horn antenna (15 dBi), L_{Probe} is probe loss (2.0 dB), L_{Adapter} is waveguide to coax adapter loss (0.35 dB), λ is the free-space wavelength (7.89 mm), and "R" is the distance between the horn antenna and the AUT (40 cm). The above-mentioned calculations are related to 38 GHz of frequency.

The measurements are conducted after placing the fabricated on-chip antenna over a miniature plastic slab ($5 \times 5 \times 3\ \text{mm}^3$) for the purpose of minimizing the reflections from the metallic chuck of the probe station. 3-D printed plastic slab, shown in Figure 5, is made up of poly lactic acid (PLA) material. Figure 7 depicts the simulated and measured radiation patterns of the proposed OCA captured at the center frequency of 38 GHz. In the XZ plane, the simulated radiation pattern shows a peak antenna gain of 1.6 dBi, and

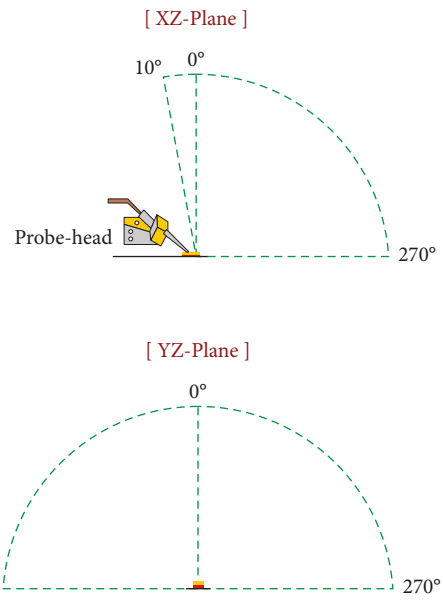

Figure 8: Scannable angular sectors for XZ plane and YZ plane.

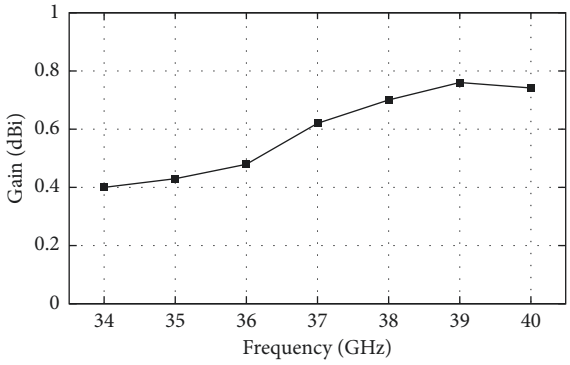

Figure 9: Measured peak gain values of the fabricated OCA at different frequencies.

the measured radiation trace exhibits the peak gain of 0.7 dBi whereas, in the YZ plane, the simulated and measured radiation traces show the peak gain values of 0.09 dBi and −0.52 dBi, respectively. It is important to note here that the proximity of the probe head to AUT limits the scanning zone of the horn antenna in the XZ plane as shown in Figure 8. The radiation pattern is scanned up to a safe limit of 10°, and the reading is not captured beyond this point. However, in the YZ plane, the entire angular sector from 90° to 270° is scanned for acquiring the radiation pattern. The tilt in the antenna beam of radiation (Figure 7(a)) confirms that the positioning of the OCA structure close to the edge of the microchip facilitates the antenna to radiate readily into free space and hence minimizes the absorption of radiation within the silicon substrate. The minor discrepancy in the simulated and measured results could be due to the reason that the OCA experienced slightly higher dielectric and conductor losses than expected.

Figure 9 depicts the measured peak gain of the fabricated OCA at different frequencies in the vicinity of 38 GHz. It can be observed from Figure 9 that the gain values are slightly higher at 39 GHz and 40 GHz as compared to 38 GHz of frequency. This can easily be explained by observing the measured reflection coefficient trace in Figure 6. The measured S_{11} trace in Figure 6 touches −15 dB at 38 GHz and continues to follow the downward trend up to 40 GHz. A better reflection coefficient value means there exists less mismatch and more power is being transferred to the OCA. This is the reason that at 39 GHz and 40 GHz, the measured gain of the antenna is coming better than at 38 GHz of frequency whereas, for frequencies below 38 GHz, as the measured reflection coefficient trace shows an upward trend (moving from 38 GHz to 32 GHz) in Figure 6, therefore, the corresponding gain values in Figure 9 are lower than that at 38 GHz of frequency.

4. Conclusion

The paper presents a 38 GHz on-chip planar inverted-F antenna (PIFA) implemented in TSMC 180 nm CMOS process node. The OCA structure is deployed with the help of the ultrathick metal (UTM) layer. For improving the gain performance, the OCA is positioned close to the edge of the microchip. The open end of the antenna is bent to develop a top-loaded PIFA structure resulting in better 50 Ω impedance matching and wider bandwidth. Measurements are conducted after placing the OCA over a 3D-printed plastic slab to reduce the reflections from the metallic chuck of the probe station. The proposed antenna showed a return loss of 14.8 dB and a gain of 0.7 dBi at the center frequency of 38 GHz. The implemented CMOS-PIFA offered a simple geometrical structure, a small form factor, and a cost-effective antenna solution. Therefore, it is one of the most suitable on-chip antennas for applications related to 5 G cellular communications at the 38 GHz band.

Data Availability

No data were used to support this study.

Conflicts of Interest

The authors declare that they have no conflicts of interest.

References

[1] H. M. Cheema and A. Shamim, "The last barrier: on-chip antennas," *IEEE Microwave Magazine*, vol. 14, no. 1, pp. 79–91, 2013.

[2] T. S. Rappaport, S. Sun, R. Mayzus et al., "Millimeter wave mobile communications for 5G cellular: it will work," *IEEE Access*, vol. 1, pp. 335–349, 2013.

[3] Y. P. Zhang, M. Sun, and L. H. Guo, "On-chip antennas for 60-GHz radios in silicon technology," *IEEE Transactions on Electron Devices*, vol. 52, no. 7, pp. 1664–1668, 2005.

[4] P. J. Guo and H.-R. Chuang, "60-GHz Millimeter-Wave CMOS RFIC On-Chip Meander-Line Planar Inverted-F Antenna for WPAN Applications," in *Proceedings of the IEEE Antennas and Propagation Society International Symposium*, pp. 1–4, San Diego, CA, USA, July 2008.

[5] D. Gang, H. M. Yang, and Y. Y. Tang, "Wideband 60-GHz on-chip triangular monopole antenna in CMOS," in *Proceedings of the 3rd Asia-Pacific Conference on Antennas and Propagation*, pp. 623–626, Harbin, China, July. 2014.

[6] H. Chu, L Qingyuan, and Y. X Guo, "60-GHz broadband CMOS on-chip antenna with an artificial magnetic conductor," in *Proceedings of the 2016 IEEE MTT-S International Microwave Workshop Series on Advanced Materials and Processes for RF and THz Applications (IMWS-AMP)*, Chengdu, China, July. 2016.

[7] P. Burasa, T. Djerafi, and K. Wu, "A 28 GHz and 60 GHz dual-band on-chip antenna for 5G-compatible IoT-served sensors in standard CMOS process," *IEEE Transactions on Antennas and Propagation*, vol. 69, no. 5, pp. 2940–2945, 2021.

[8] P. J. Guo, S. S. Hsu, C. Y. Hsu, and H. R. Chuang, "A 60-GHz Millimeter- Wave CMOS RFIC On-Chip Triangular Monopole Antenna for WPAN Applications," in *Proceedings of the IEEE Antennas and Propagation Society International Symposium*, pp. 1–4, Honolulu, HI, USA, June 2007.

[9] K. S. Sultan, H. H. Abdullah, E. A. Abdallah, M. A. Basha, and H. H. El-Hennawy, "A 60-GHz gain enhanced vivaldi antenna on-chip," in *Proceedings of the IEEE International Symposium on Antennas and Propagation & USNC/URSI National Radio Science Meeting*, pp. 1821-1822, Boston, MA, July. 2018.

[10] A. Masrouri and N. Amiri, "Circularly Polarized On-Chip Antenna for 60GHz Indoor Wireless Communications," in *Proceedings of the IEEE 18th Mediterranean Microwave Symposium (MMS)*, pp. 264–267, Istanbul, Turkey, November. 2018.

[11] S. S. Hsu, K. C. Wei, C. Y. Hsu, and R. C. Huey, "A 60-GHz millimeter-wave CPW-fed yagi antenna fabricated by using 0.18-μm CMOS technology," *IEEE Electron Device Letters*, vol. 29, no. 6, pp. 625–627, 2008.

[12] M. K. Hedayati, A. Abdipour, R. S. Shirazi, M. John, M. J. Ammann, and R. B. Staszewski, "A 38 GHz on-chip antenna in 28-nm CMOS using artificial magnetic conductor for 5G wireless systems," in *Proceedings of the 2016 Fourth International Conference on Millimeter-Wave and Terahertz Technologies (MMWaTT)*, pp. 29–32, Tehran, Iran, December 2016.